

Oxygen vacancies or/and antisite imperfections in $\text{Sr}_2\text{FeMoO}_6$ double perovskites: an *ab initio* investigation

This article has been downloaded from IOPscience. Please scroll down to see the full text article.

2005 J. Phys.: Condens. Matter 17 6415

(<http://iopscience.iop.org/0953-8984/17/41/012>)

View [the table of contents for this issue](#), or go to the [journal homepage](#) for more

Download details:

IP Address: 129.252.86.83

The article was downloaded on 28/05/2010 at 06:10

Please note that [terms and conditions apply](#).

Oxygen vacancies or/and antisite imperfections in $\text{Sr}_2\text{FeMoO}_6$ double perovskites: an *ab initio* investigation

Daniel Stoeffler¹ and Silviu Colis

Institut de Physique et de Chimie des Matériaux de Strasbourg (UMR 7504 CNRS), 23 rue du Loess, BP 43, F-67034 Strasbourg Cedex 2, France

E-mail: Daniel.Stoeffler@ipcms.u-strasbg.fr

Received 11 July 2005, in final form 30 August 2005

Published 30 September 2005

Online at stacks.iop.org/JPhysCM/17/6415

Abstract

We report on electronic band structure calculations, using the *ab initio* full potential linearized augmented plane wave (FLAPW) method, for $\text{Sr}_2\text{FeMoO}_6$ (SFMO) double perovskites presenting antisite defects or/and oxygen vacancies. We exhibit that the half-metallic character is preserved for SFMO containing only nearly isolated oxygen vacancies, indicating that the control of oxygen content in such compounds is less critical for the transport properties than the control of the antisite defects. We show that the total magnetic moment is much more reduced for structures with oxygen vacancies (approximately $2 \mu_B$ per vacancy) than for structures without. We also investigate the stability of an antiparallel (AP) magnetic moment on Fe antisites and we show that these solutions are highly unstable relative to the parallel (P) solution, even if the presence of O vacancies reduces the difference between P and AP solutions.

1. Introduction

The observation at room temperature of a large magnetoresistance in magnetic tunnel junctions [1] gave rise to an increase of the interest in these systems mainly due to their potential applications such as read heads, recording media, magnetic memories or field sensors [2]. In most junctions, CoFe alloys are used as magnetic electrodes but their polarization does not exceed 50% and leads therefore to a limited magnetoresistance. Many works focus on the increase of the sensitivity of these systems by investigating alternative materials that could be used as barriers [3] or magnetic electrodes [4]. A new direction of investigation consists in replacing the metallic electrodes by magnetic oxide having high magnetic polarization. In this context, $\text{Sr}_2\text{FeMoO}_6$ (SFMO) double perovskites are good candidates for magnetic

¹ Author to whom any correspondence should be addressed.

electrode materials for such applications because they present a half-metallic character (a 100% polarization theoretically) and a high transition temperature, $T_C = 415$ K. This suggests a potential large polarization of the conduction electrons at room temperature [5], in contrast with earlier studied manganite compounds, for which T_C is generally smaller than 350 K [6].

In the perfect crystalline structure of SFMO, Fe and Mo atoms are arranged on two equivalent body centred tetragonal sublattices and are connected through oxygen octahedra. Assuming a double-exchange mechanism for the interaction, the Fe^{3+} ($S = 5/2$) and Mo^{5+} ($S = 1/2$) magnetic moments are antiferromagnetically coupled, leading to a theoretical magnetization value of $4 \mu_B$ per formula unit. In this compound Kobayashi *et al* [5] succeeded in measuring a reasonably high magnetoresistance of 42% at low temperature (5 K), originating from the electron transport through oxygen rich grain boundaries, and a saturation magnetization of $3 \mu_B$ per formula unit. Such a low saturation magnetization was found as well by almost all authors and was attributed mainly to the disorder between Fe and Mo cations. Indeed, due to the supposed antiferromagnetic interaction of double-exchange type between the Fe and Mo sublattices of perfect SFMO, the magnetic moment of Fe (Mo) antisites, i.e. for Fe (Mo) cations situated on Mo (Fe) sites, finds itself in an antiparallel configuration with the magnetic moment of Fe (Mo) cations on the regular sites, thus reducing the saturation magnetization [7]. This model of magnetization reduction is supported by Monte Carlo calculations, which indicate an antiparallel alignment between two Fe cations separated by an oxygen atom [8]. More recently, the magnetization reduction has been associated with the reduction of the magnetic moment of Fe and Mo when the environment of these atoms is altered. This model is in agreement with the *ab initio* LMTO-ASA calculations, which indicate that the Fe–O–Fe moments have a parallel orientation which cannot reduce the total magnetic moment [9, 10]. Nevertheless, this magnetization reduction was never calculated for both types of imperfections (oxygen vacancies and antisite defect), and the band structure was reported only for SFMO with a perfect structure or with antisite defects [9–11]. In this last case the half-metallic character of the compound was reported to disappear. This leads to the conclusion that antisite defects have to be avoided in order to preserve the half-metallic properties by recovering the high saturation magnetization.

In this context, our work analyses the importance of the oxygen vacancies and antisite defect perturbation from the point of view of the magnetization reduction and of the half-metallic character. We show clearly that the half-metallic character is preserved for structures containing nearly isolated oxygen vacancies while it vanishes when antisite defects are present. Most interesting, the magnetization reduction is four times larger per oxygen vacancy ($2 \mu_B/\text{vacancy}$) than per antisite defect, in contrast with the common suggestion that a close saturation magnetization to $4 \mu_B$ per formula unit is needed in order to preserve good transport properties of SFMO. Finally, we examine the stability of solutions with an anti-aligned magnetic moment on the Fe antisite with the number of O vacancies in the cell and show that the solutions with all Fe magnetic moments parallel is always the most stable.

2. Methodology

We have calculated the band structure for the considered double-perovskite systems and the magnetic moments carried by each atom in the full potential augmented plane wave formalism (FLAPW) in the FLEUR implementation² within the generalized gradient approximation (GGA) and taking core, semi-core and valence states into account (semi-core states being required when oxygen vacancies are present, we include them in all calculations). For the

² FLEUR is an implementation of the full potential linearized augmented plane wave method freely available at <http://www.flapw.de> funded by the European Research Network Ψ_k and managed by Professor S Bluegel.

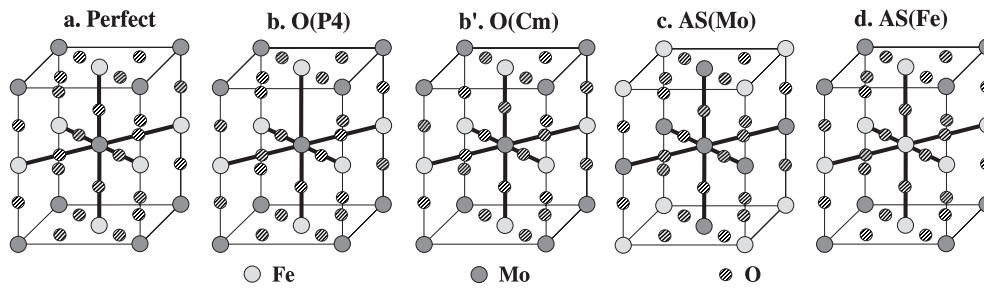


Figure 1. Representation of the five structures considered in the second section: (a) $\text{Sr}_4\text{Fe}_2\text{Mo}_2\text{O}_{12}$, perfect SFMO, (b) $\text{Sr}_4\text{Fe}_2\text{Mo}_2\text{O}_{11}$, one oxygen vacancy in a P4 in plane symmetry, (b') $\text{Sr}_4\text{Fe}_2\text{Mo}_2\text{O}_{11}$, one oxygen vacancy in a Cm in plane symmetry, (c) $\text{Sr}_4\text{FeMo}_3\text{O}_{12}$, Mo antisite defect, and (d) $\text{Sr}_4\text{Fe}_3\text{MoO}_{12}$, Fe antisite defect (for simplicity, the Sr atoms are not shown).

perfect SFMO case, the considered crystalline structure is tetragonal within the $I4/mmm$ space group, with the lattice parameters $a = 5.58 \text{ \AA}$ and $c = 7.90 \text{ \AA}$, found experimentally by x-ray diffraction [12]. For cases with imperfections, the same lattice parameters have been used but, depending on the position of the imperfection site, a lower symmetry space group has been used. Four situations were considered,

- (i) SFMO with a perfect crystalline structure,
- (ii) SFMO with a single imperfection (Mo or Fe antisite defect, oxygen vacancy),
- (iii) SFMO with two imperfections (Mo or Fe antisite defect and an oxygen vacancy, two oxygen vacancies),
- (iv) SFMO with three imperfections (Mo or Fe antisite defect and two oxygen vacancies),

in order to detect any variation which could lead to a reduction of the total magnetic moment such as the one observed. We assume that no structural relaxation occurs when imperfections are taken into account. This assumption is supported by the large total energy differences obtained during this work, which would be only slightly affected by relaxations. The self-consistent calculations were performed with sets of increasing numbers of special \mathbf{k} points until no significant variations in the charge, the magnetic moments and the total energy difference values were obtained.

3. Cases with one imperfection

Up to now, only Fe or the Mo intersite defects have been considered [9, 11], leading to the conclusion that the half-metallic character is highly sensitive to such kinds of imperfections. This is not very surprising because several Fe–O–Mo bonds are affected by such defects. For example, in the antisite considered in this section (figure 1), half of the X–O–Y bonds in the unit cell become X–O–X ($X, Y = \text{Fe or Mo}$).³ In contrast, one oxygen vacancy concerns only one X–O–Y bond and has consequently a more limited effect on the concerned atoms. This is the basic reason for which the electronic structure should be less affected by the introduction of an oxygen vacancy than by an antisite defect.

The total densities of states, displayed in figure 2, show clearly that this argument applies only for the majority spin: the minority spin electronic structure is much more affected by imperfections than the majority spin one. Consequently, the half-metallic character remains

³ The central X site $(1/2, 1/2, 1/2)$ has only X–O–X bonds, the xy plane metallic neighbour $(0, 0, 1/2)$ has four X–O–X and two X–O–Y bonds, and the z direction neighbour $(1/2, 1/2, 0)$ has two X–O–X and four X–O–Y bonds; only the $(0, 0, 0)$ atom keeps six X–O–Y bonds with its neighbours.

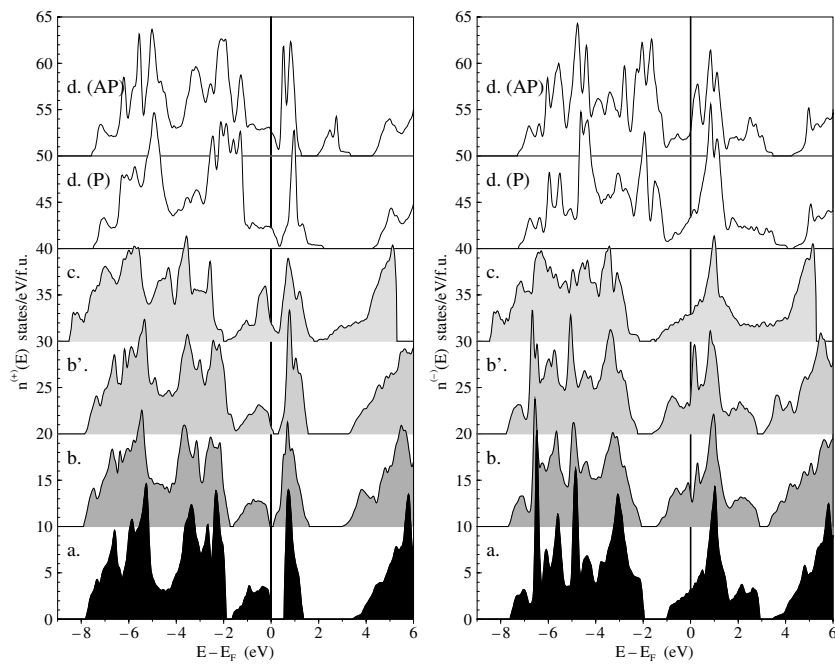


Figure 2. Majority (left) and minority (right) spin total densities of states for all five structures considered in the second section. Each curve has been offset by 10 states/eV per formula unit (f.u.) relative to the previous one and the vertical line corresponds to the Fermi level.

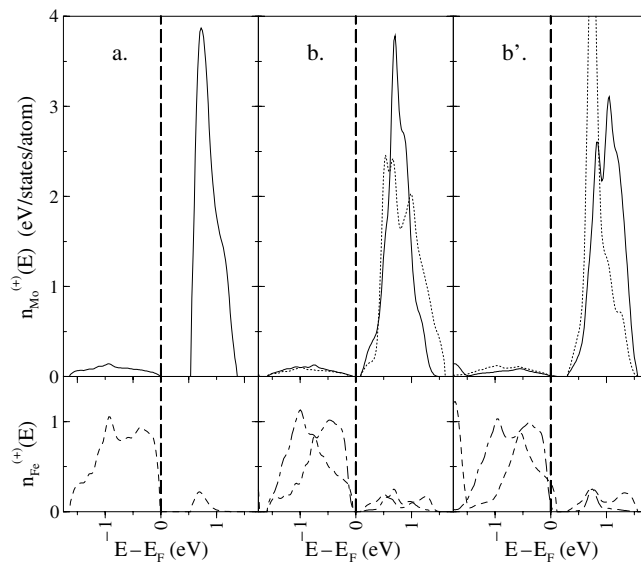


Figure 3. Majority spin Fe and Mo atom projected densities of states for structures (a), (b) and (b'): site (0, 0, 0) solid line, site (1/2, 1/2, 1/2) dotted line, site (1/2, 1/2, 0) dashed line, site (0, 0, 1/2) dot-dashed line. The thick vertical long-dashed line corresponds to the Fermi level.

for an oxygen vacancy with a reduced gap $E_g = [-0.06, 0.10]$ eV into the majority spin band as compared to the perfect SFMO $E_g = [-0.04, 0.55]$ eV. A close look at the majority spin

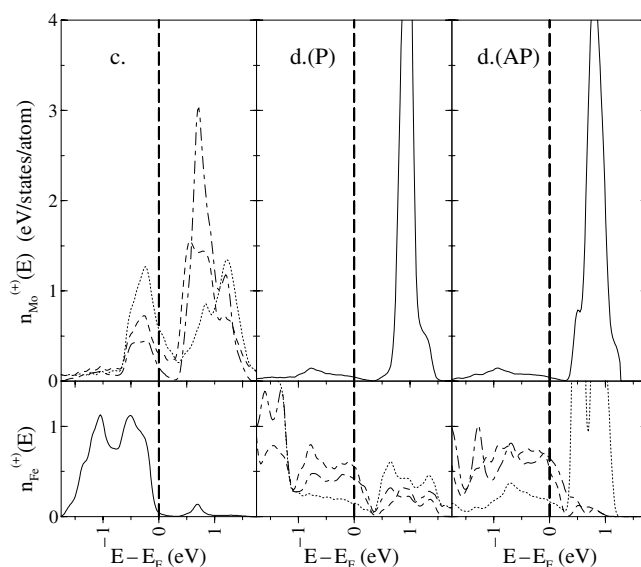


Figure 4. Majority spin Fe and Mo atom projected densities of states for structures (c) and (d): site (0, 0, 0), solid line; site (1/2, 1/2, 1/2), dotted line; site (1/2, 1/2, 0), dashed line; site (0, 0, 1/2), dot-dashed line. The thick vertical long-dashed line corresponds to the Fermi level.

total densities of states (TDOSs) (figures 3 and 4) shows clearly that the reduction of the gap for an oxygen vacancy comes mainly from a broadening of the Mo states above the Fermi energy, whereas for the antisite case the SFMO gap is mainly filled by states of the most represented atom. In contrast, the minority spin TDOSs around the Fermi level are closer to the perfect SFMO ones for the antisites than for the oxygen vacancy.

The total moment M_{tot} in the unit cell, which corresponds to the saturation magnetization of the samples, is highly affected by these imperfections. Usually, it is assumed that the observed reduced saturation magnetization results from the occurrence of antiparallel (AP) aligned magnetic moment on the Fe antisite. By starting from such an AP magnetic configuration, we could converge into a metastable solution presenting, as expected, a strongly reduced M_{tot} value. However, the total energy of this AP state is more than 0.7 eV/(anti-aligned antisite) larger than the ground state where all Fe moments are parallel. Consequently, the occurrence of such an AP magnetic configuration is very improbable.

The occurrence of an oxygen vacancy (b) or of an Fe antisite defect (d) reduces respectively M_{tot} by $2 \mu_{\text{B}}$ and $1 \mu_{\text{B}}$ with respect to the perfect cell: this M_{tot} reduction comes mainly from a negative variation of the local magnetic moments on the atoms directly concerned by the defect, i.e. the Mo and Fe atoms of the broken Fe–O–Mo bond for case (b) and the Fe excess antisite and its Fe neighbours for case (d) (see tables 1 and 2). Only a Mo excess antisite (c) gives an increase of M_{tot} by $0.81 \mu_{\text{B}}$ coming mainly from the reversal of the local magnetic moments on the Mo antisite and first Mo neighbours of the antisite. However, if we assume that we should always have pairs of Mo and Fe excess antisites, the reduction of M_{tot} becomes equal to $0.19 \mu_{\text{B}}$ for each pair. Consequently, the magnetization reduction originating from antisites remains small for a reasonable antisite concentration.

The essential role played by the delocalized electrons has been discussed recently [9]. It exhibits that the antiferromagnetic coupling between Fe and Mo magnetic moments originates mainly from a kinetic energy mechanism due to the polarization of the delocalized states. The

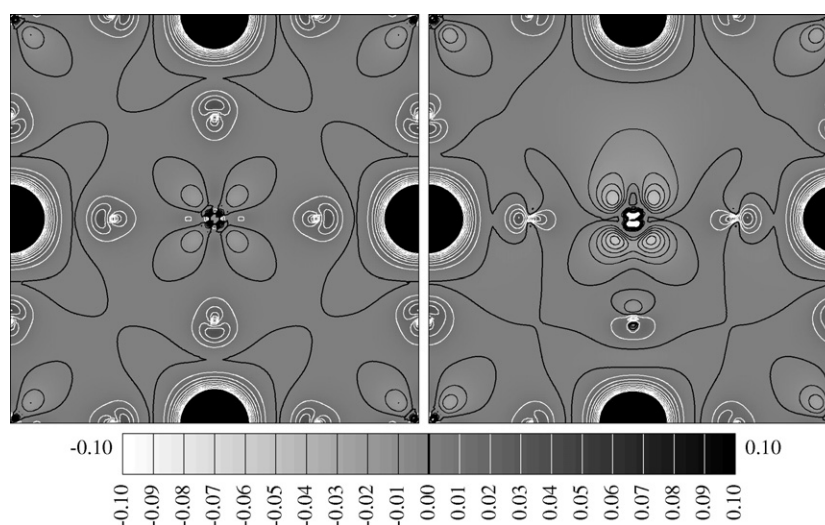


Figure 5. Spin density (in me/bohr^3) distributions in the (110) plane for case (a) (left) and case (b) (right). The Mo atoms are located in the corners and in the centre of the square, the Fe atoms correspond to the large black circular domains and the O atoms are located in the middle of each Fe–Mo bond. Positive (negative) equi-density lines are plotted in white (black) and the line of zero spin density is the thick black one.

introduction of an oxygen vacancy, which corresponds to removing one O^{2-} atom, should alter significantly the number of delocalized electrons and affect (i) the strength of the Fe–Mo coupling and (ii) the magnitude of the localized moments. A close look at the charge shows that an oxygen muffin tin sphere (whose radius is equal to 1.4 bohr) contains 6.5 electrons. Consequently, by removing one oxygen atom per cell 1.5 electrons delocalized or localized on other atoms are also removed. The calculation shows that these 1.5 electrons are nearly entirely removed from the interstitial charge. This leads us to the conclusion that an oxygen vacancy affects weakly the charge carried by the atoms. In order to discuss the role of an oxygen vacancy in the magnetic properties, the spin density distribution in the (110) plane containing all kinds of Fe, Mo and O atoms is displayed in figure 5 for cases (a) and (b). The spin density around the central Mo atom (having the O vacancy in its neighbourhood) is significantly more altered by the oxygen vacancy than around the corresponding Fe atom, whose bond to this Mo atom is removed. More explicitly, the tetragonal symmetry of the spin density around this Mo atom is completely lost. We conclude that most of the 1.5 electrons given by the oxygen atoms are delocalized and not transferred to other atoms: this confirms that they certainly play an important role in the Fe–Mo bond.

These calculations lead us to the conclusion that the observed magnetization cannot be explained by antisite imperfections because the reduction is too small for parallel moments and the solution with anti-aligned Fe moments is highly unstable. If we assume that the loss of magnetization finds its origin in imperfections of the SFMO phase, the occurrence of oxygen vacancies is clearly a candidate for accounting for it and cannot be neglected.

4. Cases with more imperfections

In order to examine a possible magnetization reduction resulting from a combination of oxygen vacancies and Fe antisites, we have studied particular cases having two oxygen vacancies (figure 6(e)), one oxygen vacancy on the octahedra surrounding the Fe antisite (figure 6(f))

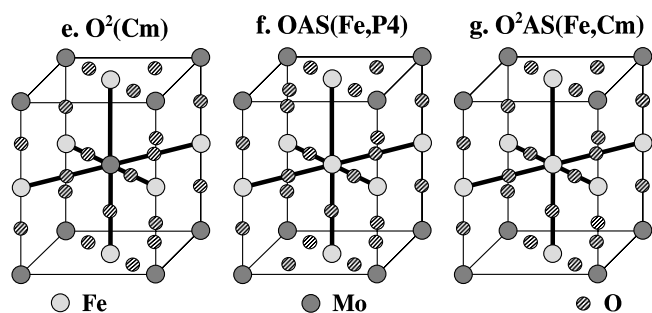


Figure 6. Representation of the three structures considered in the second section: (e) $\text{Sr}_4\text{Fe}_2\text{Mo}_2\text{O}_{10}$, two oxygen vacancies in a Cm in plane symmetry, (f) $\text{Sr}_4\text{Fe}_3\text{MoO}_{11}$, one oxygen vacancy and an Fe antisite defect in a P4 in plane symmetry, and (g) $\text{Sr}_4\text{Fe}_3\text{MoO}_{10}$ two oxygen vacancies and an Fe antisite defect in a Cm in plane symmetry (for simplicity, the Sr atoms are not shown).

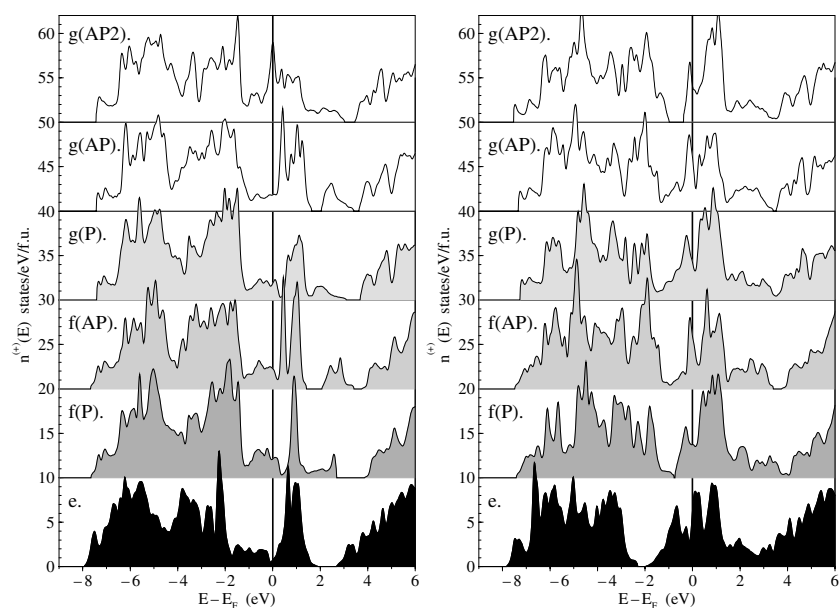


Figure 7. Majority (left) and minority (right) spin total densities of states for all three structures considered in the second section. Each curve has been offset by 10 states/eV per formula unit (f.u.) relative to the previous one and the vertical line corresponds to the Fermi level.

and two oxygen vacancies on the octahedra surrounding the Fe antisite (figure 6(g)). Case (f) can be reasonably supposed to be probable because vacancies are well known to favour the atomic mobility inside compounds and it is reasonable to assume that a vacancy and an antisite form a pair of neighbours. The two other cases are certainly less probable because a too high concentration of oxygen vacancies is required. However, it is interesting to examine this poorly probable cases in order to have the possibility to discuss extreme situations.

For an unknown reason, it was not possible to converge the high symmetry case where two oxygen vacancies are along the same z direction. This is why we consider only the case where one oxygen vacancy lies in the xy plane and the other in the z direction corresponding to a combination of cases (b) and (b'). This case with two oxygen vacancies (e) is no longer

Table 1. Calculated local magnetic moment (in μ_B) carried by the Fe, Mo and O atoms and total magnetic moment M_{tot} (in μ_B) in the cell in structures (a), (b) and (b') displayed in figure 1 (for case a, one cell corresponds to two formula units). The number of equivalent sites and the position of one atom are given (respectively between square brackets and parentheses) for each group of equivalent sites.

Cell	(a)	(b)	(b')
Fe	+3.77 _[2]	+3.41 _{[1](1/2,1/2,0)} +3.72 _{[1](0,0,1/2)}	+3.32 _{[1](1/2,1/2,0)} +3.75 _{[1](0,0,1/2)}
Mo	-0.28 _[2]	-0.41 _{[1](0,0,0)} -0.74 _{[1](1/2,1/2,1/2)}	-0.80 _{[1](0,0,0)} -0.36 _{[1](1/2,1/2,1/2)}
O		+0.06 _{[4](1/4,1/4,0)}	+0.04 _{[2](1/4,3/4,0)} +0.01 _{[1](3/4,3/4,0)}
	+0.08 _[12]	+0.09 _{[1](0,0,1/4)} +0.04 _{[1](1/2,1/2,1/4)} +0.05 _{[4](1/4,1/4,1/2)} +0.05 _{[1](0,0,3/4)}	+0.06 _{[2](1/2,1/2,1/4)} +0.06 _{[2](0,0,1/4)} +0.08 _{[2](1/4,3/4,1/2)} +0.08 _{[1](3/4,3/4,1/2)} +0.07 _{[1](1/4,1/4,1/2)}
M_{tot}	8.00	6.00	5.89

half metallic and the gap near the Fermi level disappears completely: the states coming from the Fe and Mo sites having an oxygen vacancy in the xy plane as neighbours are at the origin of this disappearance. A minimum of the density of states (figure 7(e)) at the Fermi level, reminiscent of the half-metallic character, preserves however a high polarization. Similarly to the cases with only one vacancy, 1.5 supplementary electrons are removed from the interstitial charge, leading to the conclusion that the 1.5 electrons given by the oxygen atoms are always delocalized. The total magnetic moment is found to be equal to $4.16 \mu_B$, giving a reduction of nearly $2 \mu_B$ per oxygen vacancy resulting from the nearly half-metallic character of this system. It is interesting to note that oxygen vacancies result in a significative reduction of the local moment carried by Fe atoms and a large augmentation of that carried by the Mo atoms (up to a factor of three). This could be confirmed experimentally by measuring the Mo local moment in oxygen controlled non-stoichiometric samples.

As discussed in the previous section, the solution with an antiparallel local magnetic moment on the Fe intersite is highly unstable for case (d). Consequently, the Fe–O–Fe links strongly favours a parallel coupling between the magnetic moments of the Fe atoms. Introducing one vacancy into the cell allows us to break one of these links, removing 1.5 electrons from the delocalized charge, and could therefore stabilize antiparallel solutions. This trend is effectively obtained but the solutions where all Fe magnetic moments are parallel always remains the most stable. Indeed, the energy difference between the P and AP solutions is approximately divided by two as compared to case (d): it is equal to $0.36 \text{ eV}/(\text{anti-aligned antisite})$ for case (f) and to $0.31 \text{ eV}/(\text{anti-aligned antisite})$ for case (g). Case (g) allows us to consider an extra solution (denoted by AP2) where the AP local magnetic moment is not carried by the antisite but by the Fe atom having one Fe–O–Fe bond missing in the z direction and one Fe–O–Mo bond missing in the xy plane (see figure 6(g)). For this AP2 solution, the Mo magnetic moment is found to be positive ($+0.63 \mu_B$) (see table 3): this can be understood in terms of the competition between two Fe–O–Mo bonds (in the z direction) with a positive Fe moment and three Fe–O–Mo bonds (in the xy plane) with a negative Fe moment, won by the latter. Consequently, a large total moment of $4.84 \mu_B$, as compared to the AP solution, is obtained. The total energy difference is also reduced and is equal to $0.19 \text{ eV}/(\text{anti-aligned})$

Table 2. Calculated local magnetic moment (in μ_B) carried by the Fe, Mo and O atoms and total magnetic moment M_{tot} (in μ_B) in the cell for structures (c) and (d) displayed in figure 1. For case (d) the two values correspond respectively to a parallel (P) or antiparallel (AP) local magnetic moment on the Fe antisite relative to the total magnetic moment. The number of equivalent sites and the position of one atom are given (respectively between square brackets and parentheses) for each group of equivalent sites.

Cell	(c)	d(P/AP)
Fe	+3.78 _{[1](0,0,0)}	+3.40/+3.65 _{[1](1/2,1/2,0)} +3.22/+3.42 _{[1](0,0,1/2)} +2.98/−3.20 _{[1](1/2,1/2,1/2)}
Mo	−0.14 _{[1](1/2,1/2,0)} +0.07 _{[1](0,0,1/2)} +0.33 _{[1](1/2,1/2,1/2)}	−0.14/−0.05 _{[1](0,0,0)}
O	+0.08 _{[4](1/4,1/4,0)} +0.10 _{[2](0,0,1/4)} +0.01 _{[2](1/2,1/2,1/4)} +0.00 _{[4](1/4,1/4,1/2)}	+0.06/+0.07 _{[4](1/4,1/4,0)} +0.05/+0.06 _{[2](0,0,1/4)} +0.14/+0.07 _{[2](1/2,1/2,1/4)} +0.14/+0.04 _{[4](1/4,1/4,1/2)}
M_{tot}	4.81	11.00/4.63

Table 3. Calculated local magnetic moment (in μ_B) carried by the Fe, Mo and O atoms and total magnetic moment M_{tot} (in μ_B) in the cell for structures (e), (f) and (g) displayed in figure 6. For cases (f) and (g), the three values correspond respectively to a parallel (P) or antiparallel (AP, AP2) local magnetic moment on the Fe antisite relative to the total magnetic moment. The number of equivalent sites and the position of one atom are given (respectively between square brackets and parentheses) for each group of equivalent sites.

Cell	(e)	f(P/AP)	g(P/AP/AP2)
Fe	+2.90 _{[1](1/2,1/2,0)} +3.70 _{[1](0,0,1/2)}	+3.46/+3.36 _{[1](1/2,1/2,0)} +2.98/+3.37 _{[1](0,0,1/2)} +3.15/−3.46 _{[1](1/2,1/2,1/2)}	+3.11/+2.91/−2.89 _{[1](1/2,1/2,0)} +3.02/+3.35/+2.89 _{[1](0,0,1/2)} +3.14/−3.47/+3.06 _{[1](1/2,1/2,1/2)}
Mo	−0.89 _{[1](0,0,0)} −0.73 _{[1](1/2,1/2,1/2)}	−0.28/−0.37 _{[1](0,0,0)}	−0.79/−0.86/+0.63 _{[1](0,0,0)}
O	+0.00 _{[2](1/4,3/4,0)} +0.00 _{[1](3/4,3/4,0)} +0.06 _{[1](0,0,1/4)} +0.04 _{[1](1/2,1/2,1/4)} +0.05 _{[1](1/4,1/4,1/2)} +0.05 _{[2](1/4,3/4,1/2)} +0.05 _{[1](3/4,3/4,1/2)} +0.05 _{[1](0,0,3/4)}	+0.07/+0.07 _{[4](1/4,1/4,0)} +0.06/+0.05 _{[1](0,0,1/4)} +0.28/+0.00 _{[1](1/2,1/2,1/4)} +0.13/−0.03 _{[4](1/4,1/4,1/2)} +0.02/+0.03 _{[1](0,0,3/4)}	+0.01/+0.02/−0.01 _{[2](1/4,3/4,0)} +0.01/+0.02/−0.01 _{[1](3/4,3/4,0)} +0.05/+0.04/+0.04 _{[1](0,0,1/4)} +0.26/+0.01/−0.04 _{[1](1/2,1/2,1/4)} +0.12/−0.05/+0.13 _{[1](1/4,1/4,1/2)} +0.13/−0.04/+0.13 _{[2](1/4,3/4,1/2)} +0.12/−0.05/+0.12 _{[1](3/4,3/4,1/2)} +0.01/+0.02/+0.04 _{[1](0,0,3/4)}
M_{tot}	4.16	10.66/3.06	8.92/1.22/4.84

AP2 site). All these differences remain too large to expect that atomic relaxations (which are not taken into account in the present work) can reverse the relative stability of P and AP solutions. The densities of states (figure 7) are clearly metallic-like, reinforcing the feeling that ferromagnetism is strongly favoured in our systems. Consequently, for an Fe antisite, an AP solution more stable than a P solution cannot be obtained with such kinds of calculations.

Previously, we have shown that the total magnetic moment is reduced by approximately $2 \mu_B$ per oxygen vacancy without antisites resulting from a combined decrease of the Fe local magnetic moment and increase of the magnitude of the negative Mo local magnetic moment. With an Fe antisite, the reduction is significantly smaller for the P solutions when oxygen

vacancies are included (it is found equal to $0.34 \mu_B$ for one oxygen vacancy (case f) and to $2.08 \mu_B$ for two oxygen vacancies (case g)) because there is only one Mo atom in the cell where two Mo atoms were present previously. Consequently, an oxygen vacancy combined with an antisite pair reduces the total magnetic moment four times less than an isolated vacancy. For the AP solutions, the total magnetic moment is found to decrease by approximately $1.6 \mu_B$ per vacancy.

5. Conclusion

We have shown that the half-metallic feature is easily lost in presence of imperfections, only a low concentration of O vacancies preserving this feature. We have also shown that for Fe antisites, the solutions where all Fe local magnetic moments are parallel aligned are the most stable whatever the nature of the imperfection is (with or without oxygen vacancies). This seems to be a major lack of such kinds of calculations because several studies introduce anti-aligned local moments on the Fe antisites in order to explain their results. Our calculation shows that each Mo–(AP Fe) pair of antisites reduces the total moment by $6.56 \mu_B$: in order to account for the experimental reduction of $1 \mu_B$ per formula unit, an Fe antisite concentration around 15% is required. We have also shown that the total magnetic moment reduction due to imperfections is small except for nearly isolated oxygen vacancies, where the reduction is around $2 \mu_B$ per vacancy. Consequently, oxygen vacancies could be an alternative explanation of the observed reduced magnetization if we assume a vacancy concentration of 8.5%.

One major limitation of our study comes from the high concentration of interstitials, due to the use of small cells, resulting in having planes containing only Fe atoms alternating with planes containing Mo and Fe atoms. This enhances the metallic character in our system and could be the reason why AP solutions become highly unstable. This is why future work will concern larger cells in order to model more isolated Fe antisites. In the same type of idea, to reinforce the half-metallic character, the modifications due to the use of the LDA + U [13] approach will be investigated in the future.

Acknowledgments

The authors thank A Dinia, P Panissod and G Pourroy for stimulating discussions and the Centre d'Etudes du Calcul Parallèle et de la Visualisation (<http://www-cecpv.u-strasbg.fr>) of Louis Pasteur University for computing facilities.

References

- [1] Moodera J S, Kinder L R, Wong T M and Meservey R 1995 *Phys. Rev. Lett.* **74** 3273
- [2] Prinz G A 1999 *Science* **282** 1660
- [3] Dimopoulos T, Gieres G, Colis S, Wecker J, Luo Y and Samwer K 2003 *Appl. Phys. Lett.* **83** 3338
- [4] De Teresa J M, Barthelemy A, Fert A, Contour J P, Montaigne F and Seneor P 1999 *Science* **286** 507
- [5] Kobayashi K I, Kimura T, Sawada H, Terakura K and Tokura Y 1998 *Nature* **395** 677
- [6] Gupta A and Sun J Z 1999 *J. Magn. Magn. Mater.* **200** 24
- [7] Balcells L, Navarro J, Bibes M, Roig A, Martinez B and Fontcuberta J 2001 *Appl. Phys. Lett.* **78** 781
- [8] Ogale A S, Ogale S B, Ramesh R and Venkatesan T 1999 *Appl. Phys. Lett.* **75** 537
- [9] Saha-Dasgupta T and Sarma D D 2001 *Phys. Rev. B* **64** 064408
- [10] Sarma D D 2000 *Phys. Rev. Lett.* **85** 2549
- [11] Solovyev I V 2002 *Phys. Rev. B* **65** 144446
- [12] Colis S *et al* 2005 *J. Appl. Phys.* **98** 033905
- [13] Wu H 2001 *Phys. Rev. B* **64** 125126